Structure Analysis of Sulfated Polysaccharides Extracted from *Scinaia interrupta*: A Experimental and Density Functional Theory Studies

NIVEDITA ACHARJEE[iD] and TUHIN GHOSH[*,iD]

Department of Chemistry, Durgapur Government College, Durgapur-713214, India

*Corresponding author: Tel./Fax: +91 34 32500534; E-mail: tuhinghoshbuchem@gmail.com

In present report, a combined experimental and theoretical study has been performed to address the isolation procedure and spectroscopic structure elucidation of polysaccharides such as xylomannan isolated from marine red algal source *Scinaia interrupta*. The structure of the polysaccharides obtained from the red algae of *Scinaia interrupta* has been studied from NMR, IR and GC-MS spectroscopy. The investigation revealed that red algae contained a backbone of α-(1→4)-linked D-mannopyranosyl residues substituted at 6-position with a single stub of β-D-xylopyranosyl residues. The major polysaccharide, which had 0.6 sulfate groups per monomer unit and an apparent molecular mass of 120 KDa. The backbone structure was optimized at DFT/B3LYP/6-311G(d,p) level of theory and GIAO-NMR studies were performed at B3LYP/6-311++G(2d,p) level of theory followed by mean absolute error calculations of the computed chemical shifts for two possible conformers resulting from the flipping of xylopyranosyl residue. The NMR calculations were in agreement with the experimental findings. The experimental ^{1}H NMR chemical shifts were then correlated with the NBO, Merz Kollman (MK), ChelpG and Mulliken charges of the predicted conformer. A reasonable correlation with the experimental ^{1}H NMR chemical shifts and the computed NBO charges with correlation coefficient of 0.906.

Keywords: *Scinaia interrupta*, Marine algae, Polysaccharides, Size exclusion chromatography, Density functional theory.

INTRODUCTION

The sulfated xylomannans are the class of polysaccharides that contain substantial amount of D-xylomannan and sulfated ester groups, which are found in the red algae and some marine invertebrates [1,2]. The backbone of sulfated xylomannans is made up of (1→3)-linked mannopyranosyl backbones that are partially substituted at C-2 and/or C-4 with sulfate groups and xylopyranosyl residues at C-6 [3]. The algal source also contains galactose, glucose, and glucuronic acid as minor components, which has been reported in some cases [4,5]. These complex polysaccharides depict a wide range of biological activities, such as antiadhesive [6], antiproliferative [7], anticoagulant [8], antithrombic [9] and antiplatelet-aggregation properties [10], among others. In particular, sulfated xylomannans were found to be inhibitors of human pathogenic enveloped viruses including HIV, herpes simplex virus (HSV) and human cytomegalovirus (HCMV) [11-13]. However, the structural features of sulfated xylomannans responsible for these biological activ-

ities have not been determined. Most of the difficulties for these studies may be related to the reported diverse, complex and heterogeneous structures of this kind of polysaccharides [5, 14]. In fact, the xylomannan sulfate isolated from red seaweed is found to exist as a mixture of molecules with different structures [13,15]. To further study the biological properties of xylomannan, isolation of pure xylomannan is necessary with well defined structures to establish structure activity relationships. To sum up, we may conclude that that it is quite challenging and time consuming by modern spectroscopy techniques to characterize complicated polysaccharide structures as well as their conformers which express differently bioactivities.

Since the last decade, computational approaches have been gaining interest for the purpose of deducing and conforming the structure of organic compounds. This method involves a comparison of theoretical computational data with the experimental data obtained by ^{1}H NMR chemical shift measurements for each proposed structure. The computational calculations validates the proposed experimental structure of the compounds

of interest along with molecular conformer distribution analyzes. There is no previous report of computational work which computed the structures of seaweed sulfated xylomannan polysaccharides from Scinaia genus. A known method of density functional theory (DFT) has been used to determine structures of xylomannan extracted from red seaweed *Scinaia interrupta* in this work to provide a different way of confirming the structural determination of the polysaccharide by ^{1}H NMR spectroscopic method. The difference of the computed and experimental chemical shifts allows investigating the conformational analysis and confirming the suggested experimental structures of the sulfated polysaccharides for the first time in literature. Atomic charges cannot be obtained from experiments because the electrons show diffuse charge distribution with respect to the nuclei. These charges may possibly be derived using quantum mechanics. Comparison of different theoretical concepts for atomic charge calculations and their correlation with the experimental chemical shifts provides the prediction of appropriate charge calculation concept for different classes of compounds [16]. Such comparison and the extent of correlation between experimental chemical shifts and atomic charges have not been reported for polysaccharide structures. With this in mind, four types of atomic charges, (ESP) charges following Merz-Kollman (MK) [17] and ChelpG algorithms [18], Mulliken charges and natural bond orbital (NBO) charges [19] were calculated and correlated with the experimental ^{1}H NMR chemical shifts of the polysaccharide backbone structure.

In the present paper, the isolation, structural elucidation of xylomannan polysaccharides using spectroscopic and chemical methods and DFT study for ^{1}H NMR chemical shifts along with the correlation of experimental ^{1}H NMR chemical shifts with the atomic charges calculated using different theoretical models are reported.

EXPERIMENTAL

Plant material: Samples of *Scinaia interrupta* were collected from the Rushikonda coast, Vishakapatnam, India in October 2015. The seaweeds were washed thoroughly with tap water, dried by forced air circulation and pulverized in a blender (Waring Products Inc., Torrington, USA). Algal powder (200 g) was depigmented using sequential extraction with petroleum ether (24 h) and acetone (24 h) as solvent in a Soxhlet apparatus. The unextracted material was placed in a plastic beaker and air dried to yield depigmented algal powder (DAP; 148 g).

Extraction of sulfated xylomannan: Extraction of DAP (10 g) with water (pH 7.0) at a solute to solvent ratio of 1:100 (w/v) was conducted at 25-32 ºC for 12 h under constant stirring for three times. Separation of the residue from the extract was performed by filtration through glass filter (G-2). The residue was briefly washed with additional distilled water and the wash was collected to maximize polysaccharide recovery. The liquid extract was dialyzed extensively against water and lyophilized. The recovered material was dissolved in water; the polysaccharide were precipitated twice with ethanol (4 volumes) and then collected by centrifugation. The final pellet was dissolved in water and lyophilized to yield the water extracted polysaccharide, named A (4.8 g). The residue was further stirred with water thrice at 80 ºC for 12 h to obtain fraction B.

Size exclusion chromatography (SEC): The water extracted fraction was chromatographed on a Sephacryl S-300 column (2.6 × 90 cm; Amersham Biosciences AB, Uppsala, Sweden) using 0.5M sodium acetate buffer (pH 5.0) as eluent. The flow rate of the column was 0.5 mL/min and fractions of 10 mL were collected and checked by phenol-sulfuric acid reaction [20]. The column was calibrated with standard dextrans (500, 70, 40 and 10 kDa). Elution of polysaccharide was expressed as a function of the partition coefficient (K_{av}):

$$K_{av} = \frac{(V_e - V_0)}{(V_t - V_0)}$$

where V_t and V_o are the total and void volume of column determined as the elution volume of potassium hydrogen phthalate and dextran, respectively and V_e is the elution volume of sample.

Chemical analysis: All the chemicals used were of analytical grade. All determinations were done at least in duplicate. Evaporations were performed under diminished pressure at about 45 ºC (bath) and small volume of aqueous solutions was lyophilized. Total sugars and uronic acids were determined by the phenol-sulfuric acid [21] and *m*-hydroxydiphenyl [20] assay, respectively. For the determination of sugar composition, the monosaccharide residues released by acid hydrolysis were converted into their alditol acetate [22] and analyzed by gas-liquid chromatography (GLC; Shimadzu GC-17A, Shimadzu, Kyoto, Japan). Monosaccharides were identified by thin-layer chromatography and gas-liquid chromatography-mass spectrometry (GLC-MS; Shimadzu QP 5050 A, Shimadzu, Kyoto, Japan) as described earlier [23]. Alternatively, TMS-derivatives of methyl glycosides were analyzed by GLC [24].

Sulfate estimation and desulfation: Estimation of sulfate by the modified barium chloride method [25] and IR-spectrometry [26] and solvolytic desulfation by the method of Falshaw & Furneaux were carried out as described earlier [11].

Smith degradation: Periodate oxidation of desulfated polysaccharide (AF1D) was carried out as described by Fry [27]. Briefly, a solution of 100 mg of polysaccharide in 50 mL of reagent (50 mM $NaIO_4$ made up in 0.25 M formic acid, pH adjusted to 3.7 with 0.5 M NaOH) was incubated in the dark for 144 h at 4-6 ºC. Excess of periodate was decomposed with 10 mL ethane-1,2-diol and the solution stirred for a further 1 h period at room temperature. To a vial containing oxopolysaccharide a solution (50 mL) of 950 mg of $NaBH_4$ in 1M NaOH was added and the mixture was kept at room temperature for 12 h. The solution was subsequently neutralized with HOAc, dialyzed and lyophilized to give the oxidized and reduced polysaccharide. This preparation was hydrolyzed with TFA (pH 2) for 10 min at 100 ºC and the resulting hydrolyzate was desalted by passing through a column (2.6 × 90 cm) of Sephadex™ G-10. Fractions (5 mL) were collected and analyzed for their total sugar contents [21]. Appropriate polymeric fractions were lyophilized to afford a Smith degraded xylomannan, AF1D-Sm (58 mg).

Linkage analysis: Triethylamine form [28] of native (A), desulfated (AF1D) and desulfated Smith degraded (AF1D-

Sm) xylomannan (5 mg of each) was subjected to three rounds of methylation [29]. Permethylated samples were hydrolyzed, converted into their partially methylated alditol acetates and analyzed by GLC and GLC-MS as described [30].

Spectroscopy: Recording of IR spectra and optical rotation measurements were carried out as described [30]. The ^{1}H NMR spectra of the AF1 were recorded on a Bruker 500 spectrometer (Bruker Biospin AG, Fallanden, Switzerland) operating at 500 MHz for ^{1}H. The sulfated xylomannan was converted into sodium salt by passage through a column (7 mL, Bio-Rad, Hercules, CA, USA) of Amberlite IR 120 (H$^+$) and all samples were deuterium-exchanged by lyophilization with D_2O and then examined as 1% solutions in 99.8% D_2O.

Computational methods: Geometries of structures were optimized by density functional theory with Becke′s [31] three parameter hybrid exchange functional in combination with Lee, Yang and Parr [32] (B3LYP) using 6-311G(d,p) basis set. Thermochemical calculations were also performed on the optimized geometries at 298.15 K. (No. of imaginary frequencies = 0 for stationary states). Tran *et al*. [33] have reported optimization of the backbone structure of the polysachharides extracted from green seaweed *Ulva lactuca* at similar level of theory. GIAO/SCF NMR calculations of the optimized structures were performed at B3LYP/6-311++G(2d,p) level of theory. The hydrogen isotropic shielding values of tetramethylsilane (TMS) computed at the same level of theory was used as the reference for the respective isotropic shielding values obtained from NMR calculations of the investigated structures. Mean absolute error (MAE) [34] is a well known method to compare the experimental and computed NMR chemical shifts to determine the goodness of fit. For the present study, MAE was calculated as the average of the sum of absolute error between the computed and the experimental chemical shifts from the following formula:

$$MAE = \frac{1}{N} \sum_{i=1}^{N} \left| \delta_i^{comp} - \delta_i^{expt} \right|$$

where N is the number of unique chemical shifts, which were used for comparison.

The electronic chemical potential (μ) [35] and chemical hardness (η) were calculated from the FMO energies and the global electrophilicity index (ω) [36] was calculated from μ and η using the standard formula. NBO and ESP charges (using MK and ChelpG algorithm) were also computed for the two possible conformers. All calculations were carried out using Gaussian 2003 [37] set of programs along with the graphical interface Gauss View 2003.

Statistical analysis: Origin 6 software (Microcal Software Inc., USA) was used for data analysis. All experiments were repeated three times and data were presented as mean ± SD for three replications for each sample. The Fisher least significance test was used to check the equality of variances and oneway ANOVA was used to estimate the statistically significant difference ($p \leq 0.05$).

RESULTS AND DISCUSSION

Isolation and purification: The main goal of this study is to experimentally and theoretically identify the structural features of water extracted polysaccharides from *Scinaia interrupta*. The preliminary step is to analyze the sugar composition of the algal powder. Then it is necessary to devise a strategy for the extraction of polysaccharides based on the information obtained (Fig. 1). From the sugar composition analyses, xylose and mannose were found as major monosaccharides in the depigmented algal powder (DAP) (Table-1) and as the xylomannans are usually soluble in aqueous solvents [38-40], DAP was extracted with water. This water extracted fraction (A) amounted to 40% of DAP dry weight and is made up of mannose and xylose residues, and sulfate groups (Table-1).

For purification, size exclusion chromatographic (SEC) technique was used on a Sephacryl S-300 column, which separated A into two fractions (Fig. 2). The fraction AF1 amounted to 80% of the total polymers recovered from the column and contained mostly of mannose and xylose residues (Table-1). The major sugar mannose accounted for more than 69% of the neutral sugars of AF1, including a 5% (w/w) sulfate group. This purified polysaccharide showed a specific rotation [α]$_D^{32}$ +51° (c 0.19, H_2O), revealing that mannose and xylose residues in AF1 belongs to the D-series [39,40].

The elution profile of fraction AF1 on Sephacryl S-300 suggests that the pattern of sulfated xylomannan is homogeneous. Based on calibration with standard dextrans, the apparent
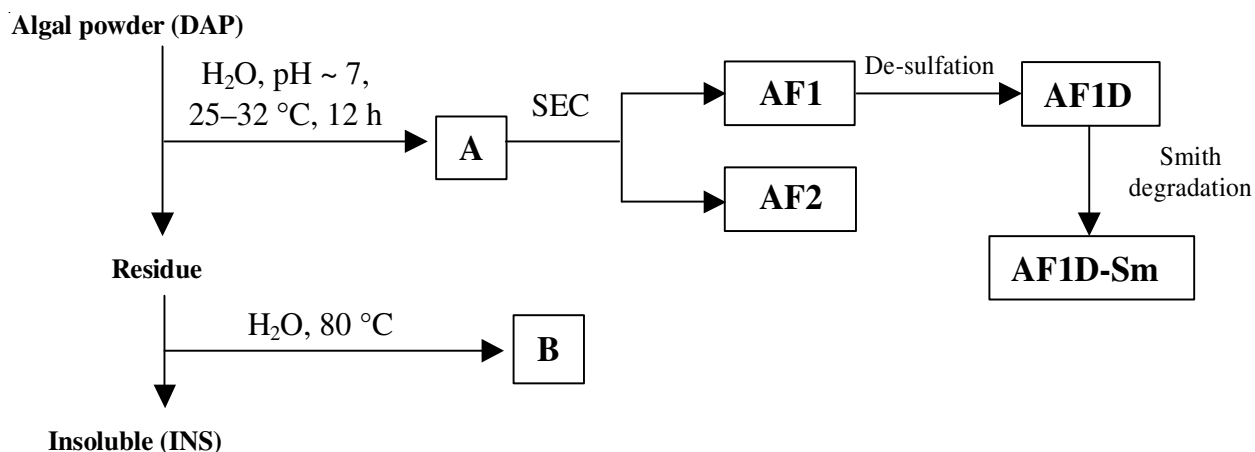

Fig. 1. Scheme for the extraction and purification of polysaccharides from marine red algae *Scinaia interrupta*

TABLE-1
SUGAR COMPOSITION (mol %) OF FRACTIONS OBTAINED FROM *Scinaia interrupta*

Fractions	A	AF1	AF2	AF1D	AF1D-Sm	B
Total sugar	43	47	35	66	42	42
Degree of sulfation	0.5	0.4	0.3	Nd	Nd	0.4
Xylose†	44	35	31	30	29	30
Mannose†	56	65	69	70	71	70

For a description of fractions see 'Experimental section'. *Percent weight of fraction dry weight. †Mol percent of neutral sugars. DS, degree of sulfation *i.e.*, numbers of sulfate group per monosaccharide residue. Nd, not determined.
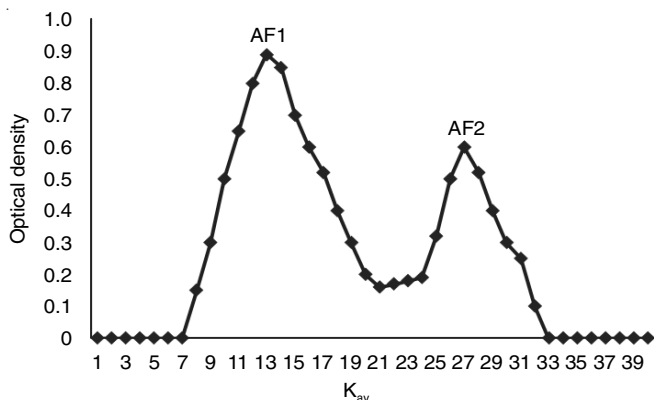
Fig. 2. Elution profile of the water extracted fraction (A) of the marine red algae *Scinaia interrupta* on Sephacryl S-300 column

molecular mass of AF1 would be 120 kDa, as determined by size exclusion chromatographic (SEC) technique.

Sulfate estimation and desulfation: The desulfation of AF1 was performed to check the role of sulfate group in the core structure of xylomanan polysaccharide from *Scinaia interrupta*. It was revealed that the solvolytic desulfation [41] gave better recovery compared to methanol-HCl and auto-desulfation method [42] from preliminary experiments (data not shown). Therefore, AF1 was desulfated by solvolysis in DMSO and the desulfated derivative (AF1D) had a recovery yield of 28%.

The FT-IR spectrum of AF1 demonstrated an intense absorption band in the region 1250 and 828 cm^{-1} associated to >S=O stretching vibration of the sulfate group [43]. In the IR spectrum of F1D, this absorbance becomes weak, demonstrated the presence of sulfate groups (Fig. 3).
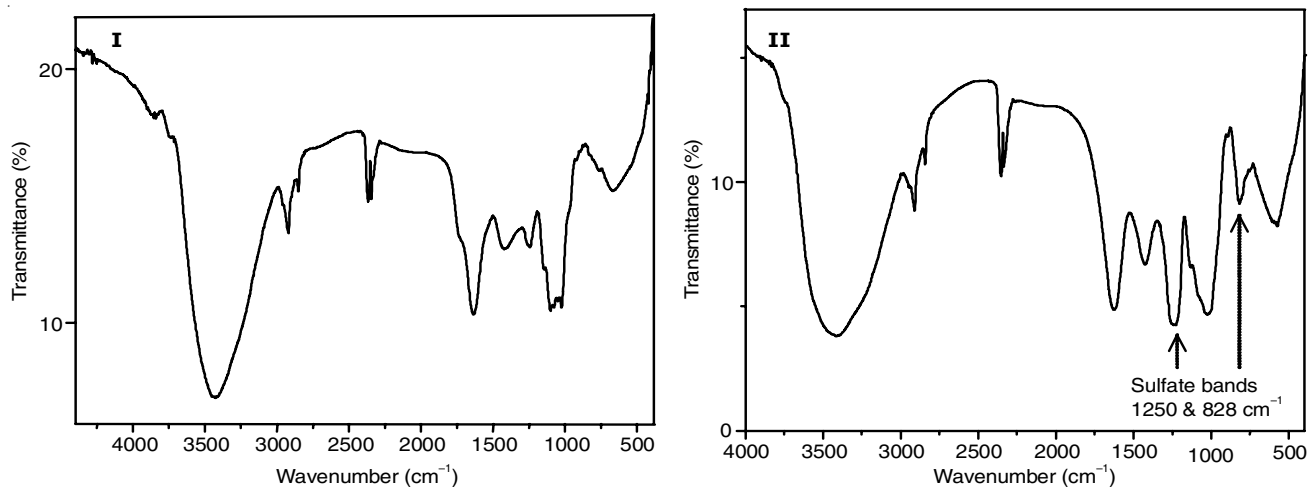
The periodic acid oxidation of F1D was performed to establish the structure of xylomannan. In this process, oxidized polymer was subsequently reduced with NaBH$_4$ and subjected to mild acid hydrolysis according to Smith degradation conditions. A Smith degraded material (AF1D-Sm) containing mannose as the only component sugar was obtained in 50% yield.

Methylation analysis: From the results of glycosidic linkage analysis of the desulfated macromolecule (AF1D), it may be predicted that 1,3,5-tri-O-acetyl-2,4,6-tri-O-methylmannitol residue is present, *i.e.* xylomannan sulfate has a (1→3)-linked backbone (Fig. 4). It was also found that a large proportion of terminal xylopyranosyl and 1,3,5,6-tetra-O-acetyl-2,4-di-O-methylmannitol residues was present, suggesting the polymer to be branched at position 6 (Table-2). The methylation analysis of native xylomannan sulfate AF1 yielded a variety of mono-, di- and trimethylated products predicting the structure to be highly complex. Consequently, an increase in the proportion of 2,4,6-tri-O-methylmannitol after desulfation, predicts that sulfate esters, when present, are located at position 6 and 2 of (1→3)-linked mannopyranosyl residues, which may be revealed from the decreased proportions of 4-O-methyl- and 2,4-di-O-methylmannitol residues.

The methylation analysis of Smith degraded polymer (AF1D-Sm) showed that the degraded polysaccharide to be a straight chain mannan built up of (1→3)-linked mannopyranosyl residues (Table-2). The disappearance of terminal-xylitol and 2,4-di-O-methyl mannitol residues suggest the presence of single stub of xylose residues at 6 position of the mannose units of native xylomannan sulfate.

NMR analysis: The sulfated xylomannan was analyzed by NMR to examine the anomeric configuration and sulfation

Fig. 3. Fourier transformed-IR spectra of (**I**) desulfated (AF1D) and (**II**) purified (AFI) xylomannan generated from *Scinaia interrupta*
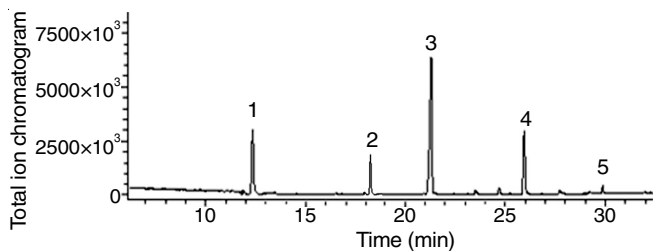
Fig. 4. Total ion chromatogram of partially methylated alditol acetates (PMAA) derived from the desulfated xylomannan (AF1D) of the red alga *Scinaia interrupta*; **1**: 1,5-di-*O*-acetyl-2,3,4-tri-*O*-methylxylitol; **2**: 1,5,6-tri-*O*-acetyl-2,3,4-tri-*O*-methylmannitol; **3**: 1,3,5-tri-*O*-acetyl-2,4,6-tri-*O*-methylmannitol; **4**: 1,3,5,6-tetra-*O*-acetyl-2,4-di-O-methylmannitol; **5**: 1,2,3,5,6-penta-O-acetyl-4-*O*-methylmannitol
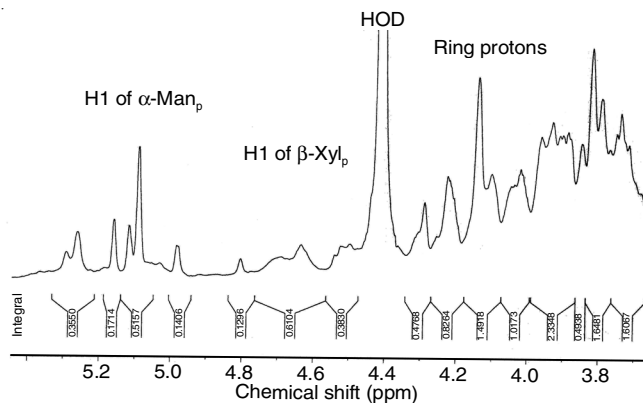

Fig. 5. ^{1}H NMR spectrum at 500 MHz of the desulfated xylomannan (AF1D) of *Scinaia interrupta*; The spectrum was recorded at 60 °C for sample in D_2O solution. The signal for the residual water was designated as HOD

TABLE-2
PARTIALLY METHYLATED ALDITOL ACETATES
DERIVED FROM NATIVE (AF1) AND DESULFATED
(AF1D) XYLOMANNAN OF *Scinaia interrupta* AND THE
SMITH-DEGRADED DERIVATIVE (AF1D-Sm)

Methylation products	Peak area[*]		
	AF1	AF1D	AF1D-Sm
2,3,4-Xyl[†]	23	27	Nd
2,3,4-Man[†]	5	3	Nd
2,4,6-Man[†]	12	48	100
2,4-Man[†]	35	20	Nd
4-Man[†]	17	2	Nd
Man[†]	8	Nd	Nd

[*]Percentage of total area of the identified peaks. [†]2,3,4-Xyl denotes 1,5-di-*O*-acetyl-2,3,4-tri-*O*-methylmannitol; *etc*. Nd, not detected.

pattern. The presence of a number of broad signals in anomeric region of ^{1}H NMR spectra of the further sulfated xylomannan suggests that their structures are very complex. The desulfated xylomannan (AF1D), on the other hand, showed only two broad anomeric resonances, one at 5.1 ppm and the other at 4.6 ppm (Fig. 5). The anomeric configuration of mannose and xylose residues of a structurally related sulfated xylomannan isolated from other red algae have been reported to be α- and β-, respec-

tively [44]. Therefore, signals at 5.1 and 4.6 ppm were tentatively assigned to anomeric protons of α-(1→3)-linked mannopyranosyl and β-linked terminal xylose residues, respectively. The relative proportion (2:1) of mannose and xylose residues as estimated from the integral of these anomeric signals fits also well with the results obtained from sugar compositional analysis. The disappearance of the later signal in the NMR spectrum of Smith degraded polymer confirms the same. Like desulfated xylomannan (AF1D), the degraded material (AF1D-Sm) also include resonances characteristic of polysaccharides such as signals from ring protons (H-2 to H-6) between 3.44 and 4.33 ppm. Therefore, NMR analysis confirmed the results of methylation analysis and indicated the presence of α-linked mannopyranosyl and β-linked terminal xylopyranosyl residues.

Analysis of global properties and computed NMR shifts: Two possible conformers A and B (Fig. 6) of the polysaccharide backbone structure were optimized during the study. A and B differ with respect to the flipping of xylopyranosyl residue, keeping the mannopyranosyl residue intact. The optimized structures are represented in Fig. 7. Table-3 listed
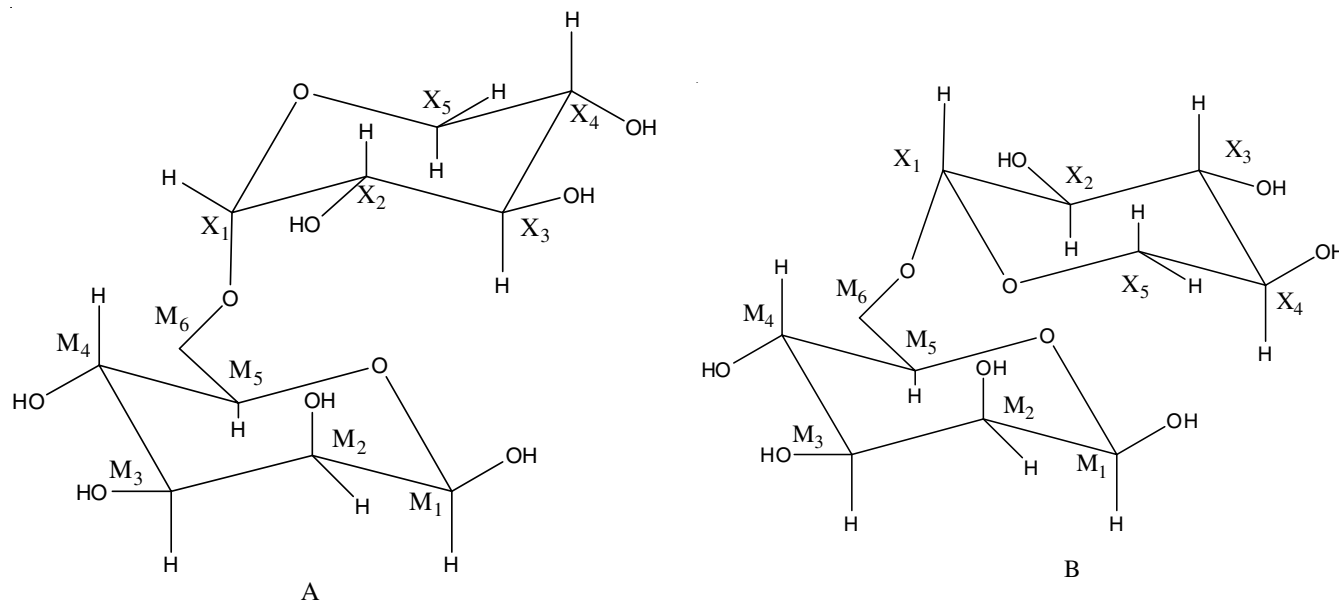

Fig. 6. Possible conformers of the polysaccharide backbone structure

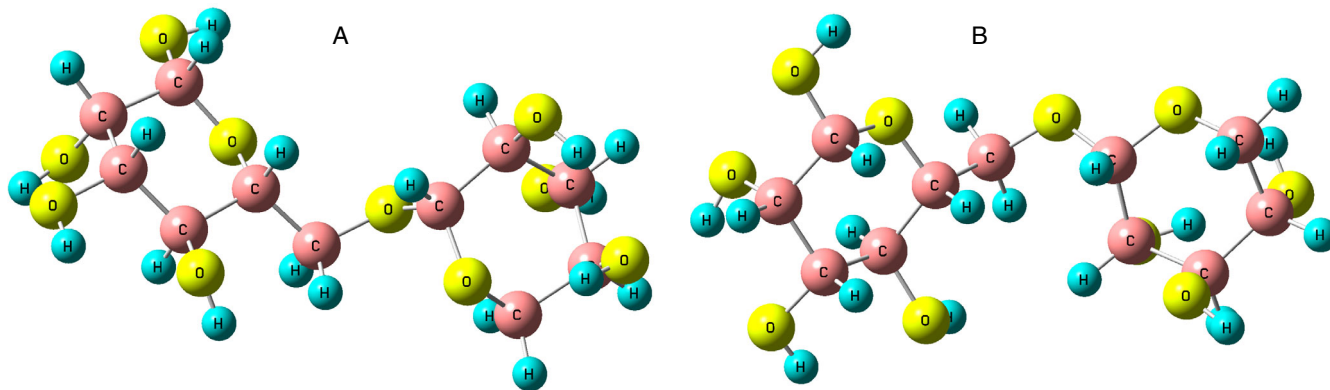| Structure	Optimized energy (au)	HOMO (eV)	LUMO (eV)	μ (eV)	η (eV)	ω (eV)
A	-1183.71570492	-7.13	0.30	-3.42	7.43	0.79
B	-1183.70731040	-6.91	0.25	-3.33	7.16	0.77

TABLE-3
GLOBAL PROPERTIES OF STRUCTURES A AND B

Fig. 7. DFT/B3LYP/6-311G(d,p) optimized structures of the possible conformers A and B

the optimized energies and global properties of structures A and B. The optimized energy of structure A is lowered by 22.04 kJ/mol compared to B. This indicates differences in the minimized optimized structure for the two conformers. Both A and B can be classified as the marginal electrophiles with the global electrophilicity ω < 0.80 eV [36]. This denotes the poor electron acceptance by both A and B in polar reactions. The HOMO-LUMO energy gap of A and B are calculated as 7.43 and 7.16 eV, respectively which is quite comparable.

In the present study, -CH protons were selected for comparison of GIAO-^{1}H NMR chemical shifts of A and B since the primary objective is to underline the differences between ^{1}H NMR chemical shifts of protons with similar multiplicity of A and B due to flipping of xylopyranosyl residue and compare them with experimentally recorded chemical shifts in terms of the mean absolute error (MAE). This comparison is shown in Fig. 8 and the corresponding data with differences and MAE value is listed in Table-4. It is evident from the graph that the computed ^{1}H NMR chemical shifts show higher values than the experimental data for both A and B. ^{1}H NMR chemical shift at M1 shows the highest value along the series. For centre X1, the ^{1}H NMR chemical shift of A differs from the experimental
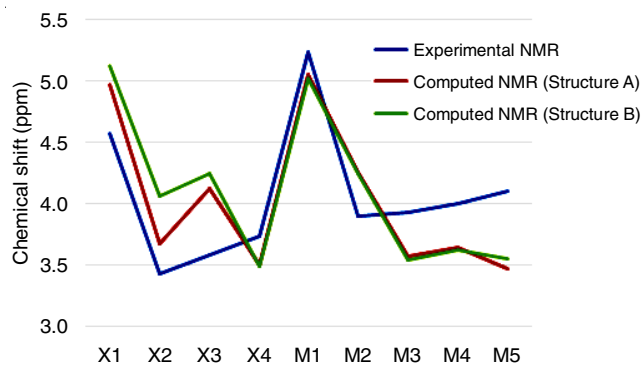
Fig. 8. Experimental and DFT/B3LYP/6-311++G(2d,p) computed ^{1}H NMR chemical shifts of A and B

value by 0.40 ppm. This difference amounts to 0.55 ppm in case of B. ^{1}H NMR chemical shifts at X2 and X3 differ by 0.25 ppm and 0.54 ppm for A, while the respective differences are calculated as 0.63 ppm and 0.67 ppm for B.

The calculated MAE for A is 0.368 and that of B is 0.443. Hence, these NMR calculations are in complete conformity with the experimentally suggested structure A for the isolated polysaccharide.

TABLE-4
DIFFERENCE IN EXPERIMENTAL AND COMPUTATIONAL ^{1}H NMR CHEMICAL SHIFTS OF STRUCTURES A AND B

Centre	δ_A exp (ppm)	Structure A		Structure B	
		δ_A comp (ppm)	δ_A comp (ppm) – δ_A exp (ppm)	δ_A comp (ppm)	δ_A comp (ppm) – δ_A exp (ppm)
X1	4.57	4.97	0.40	5.12	0.55
X2	3.43	3.68	0.25	4.06	0.63
X3	3.58	4.12	0.54	4.25	0.67
X4	3.74	3.50	0.24	3.49	0.25
M1	5.24	5.06	0.18	5.02	0.22
M2	3.90	4.25	0.35	4.25	0.35
M3	3.93	3.57	0.36	3.54	0.39
M4	4.00	3.64	0.36	3.62	0.38
M5	4.10	3.47	0.63	3.55	0.55
MAE			0.368		0.443

The correlation coefficients between the experimental chemical shifts and the atomic charges of preferred conformer A obtained from different theoretical models are shown in Fig. 9. Now, Mulliken charges are based on the total electron density basis functions of atomic centres. These charges are expected to have high basis-set dependence to provide accurate results. The shortcoming of computed charges in the Mulliken system is addressed in case of natural orbital based (NBO) charges, where charges are assigned into the atomic orbitals. The NBO based natural population analysis of the optimized structure is relatively independent of the basis set. On the other hand, electrostatic potential (ESP) charges assign the atomic charges from the molecular electrostatic potential (MEP) of the minimized structure on a three dimensional grid. Predictions from ESP charges can vary from different local minimum configurations. For the present study, the correlation coefficient between the experimental chemical shifts and NBO charges is 0.906, which is strongest among all four charges under investigation. The correlation between chemical shifts and ESP charges following Merz-Kollman and ChelpG algorithms are much weaker, the correlation coefficients are 0.696 and 0.685 respectively with much smaller R^2 of 0.484 and 0.469. In case of Mulliken charges, correlation coefficient value is 0.856 with R^2 of 0.732, which is less than that of NBO charges. Therefore, the strongest correlation is noticed between the computed NBO charges and experimental ^{1}H NMR chemical shifts of -CH protons in the polysaccharide backbone structure.

Conclusion

The present findings highlight the isolation of water extracted active polysaccharides from the red seaweed *Scinaia interrupta*. The main fraction contains a sulfated xylomannan (F1) with complex structure and a molecular mass of 120 kDa. Research

analysis showed that sulfated xylomannan from *S. interrupta* contained a backbone of α-(1→4)-linked D-mannopyranosyl residues substituted at different positions with single stub of β-D-xylopyranosyl residues and sulfate groups. Further, the polysaccharide present is highly branched, with an average of 10 branching points being present in every hundred mannopyranosyl residues. Hence, the polysaccharide described in the present work differs in structure from other known sulfated xylomannans. ^{1}H NMR calculations at DFT/B3LYP/6-311++G (2d,p) level of theory were in complete conformity with the experimentally suggested structure and showed lower mean absolute error for the preferred conformer compared to the other possible conformer. A reasonable correlation was noticed between the experimental ^{1}H NMR values and computed NBO charges with poor correlation being observed for ESP charges following Merz Kollman and ChelpG algorithms.

CONFLICT OF INTEREST

The authors declare that there is no conflict of interests regarding the publication of this article.
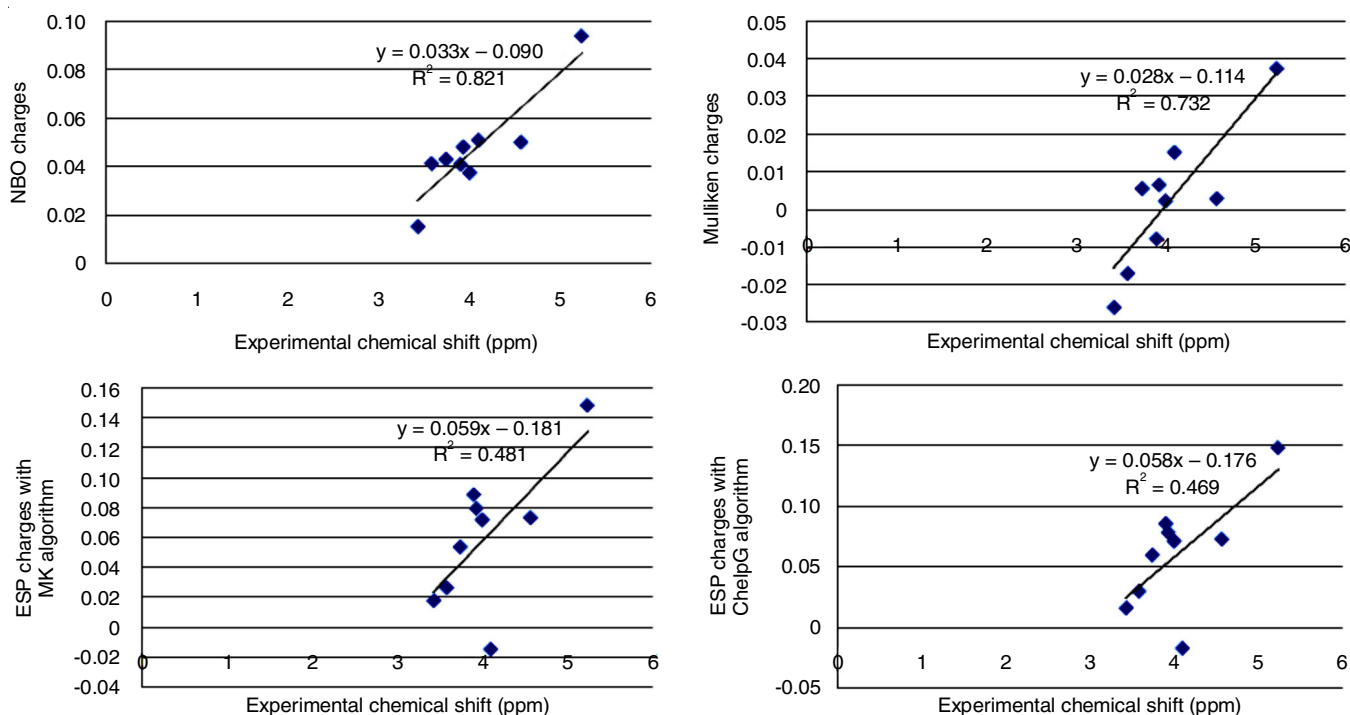

Fig. 9. Correlation of experimental ^{1}H NMR chemical shifts of preferred structure A with NBO derived, Mulliken and ESP charges

REFERENCES

1. O. Berteau and B. Mulloy, *Glycobiol.*, **13**, 29R (2003); https://doi.org/10.1093/glycob/cwg058
2. A.C.E.S. Vilela-Silva, M.O. Castro, A.P. Valente, C.H. Biermann and P.A.S. Mourao, *J. Biol. Chem.*, **277**, 379 (2002); https://doi.org/10.1074/jbc.M108496200
3. Y. Kariya, B. Mulloy, K. Imai, A. Tominaga, T. Kaneko, A. Asari, K. Suzuki, H. Masuda, M. Kyogashima and T. Ishii, *Carbohydr. Res.*, **339**, 1339 (2004); https://doi.org/10.1016/j.carres.2004.02.025
4. T. Nishino, C. Nishioka, H. Ura and T. Nagumo, *Carbohydr. Res.*, **255**, 213 (1994); https://doi.org/10.1016/S0008-6215(00)90980-7
5. T.J. Painter, ed.: G.O. Aspinall, Algal Polysaccharides: In The Polysaccharides, Academic Press: London, vol. 2, pp. 195-285 (1983).
6. S. Sattin and A. Bernardi, *Trends Biotechnol.*, **34**, 483 (2016); https://doi.org/10.1016/j.tibtech.2016.01.004
7. S. Chen, T. Yong, C. Xiao, J. Su, Y. Zhang, C. Jiao and Y. Xie, *J. Funct. Foods*, **43**, 196 (2018); https://doi.org/10.1016/j.jff.2018.02.007
8. C. Zhong, G. Cao, K. Rong, Z. Xia, T. Peng, H. Chen and J. Zhou, *Colloids Surf. B Biointerfaces*, **161**, 636 (2018); https://doi.org/10.1016/j.colsurfb.2017.11.042
9. S. Mohamed, S.N. Hashim and S.A. Rahman, *Trends Food Sci. Technol.*, **23**, 83 (2012); https://doi.org/10.1016/j.tifs.2011.09.001
10. F. Liao, A. Yu, J. Yu, D. Wang, Y. Wu, H. Zheng, Y. Meng, D. He, X. Shen and L. Wang, *J. Chromatogr. B Analyt. Technol. Biomed. Life Sci.*, **1092**, 320 (2018); https://doi.org/10.1016/j.jchromb.2018.06.027
11. T. Ghosh, K. Chattopadhyay, M. Marschall, P. Karmakar, P. Mandal and B. Ray, *Glycobiol*, **19**, 2 (2009a); https://doi.org/10.1093/glycob/cwn092
12. S.C. Feldman, S. Reynaldi, C.A. Stortz, A.S. Cerezo and E.B. Damonte, *Phytomedicine*, **6**, 335 (1999); https://doi.org/10.1016/S0944-7113(99)80055-5
13. N.M.A. Ponce, C.A. Pujol, E.B. Damonte, M.L. Flores and C.A. Stortz, *Carbohydr. Res.*, **338**, 153 (2003); https://doi.org/10.1016/S0008-6215(02)00403-2
14. M.S. Pereira, B. Mulloy and P.A.S. Mourao, *J. Biol. Chem.*, **274**, 7656 (1999); https://doi.org/10.1074/jbc.274.12.7656
15. M.E.R. Duarte, M.A. Cardoso, M.D. Noseda and A.S. Cerezo, *Carbohydr. Res.*, **333**, 281 (2001); https://doi.org/10.1016/S0008-6215(01)00149-5
16. Y. Liu, T. Junk, Y. Liu, N. Tzeng and R. Perkins, *J. Mol. Struct.*, **1086**, 43 (2015); https://doi.org/10.1016/j.molstruc.2015.01.007
17. B.H. Besler, K.M. Merz Jr. and P.A. Kollman, *J. Comput. Chem.*, **11**, 431 (1990); https://doi.org/10.1002/jcc.540110404
18. L.E. Chirlian and M.M. Francl, *J. Comput. Chem.*, **8**, 894 (1987); https://doi.org/10.1002/jcc.540080616
19. A.E. Reed and F. Weinhold, *J. Chem. Phys.*, **78**, 4066 (1983); https://doi.org/10.1063/1.445134
20. A. Ahmed and J.M. Labavitch, *J. Food Biochem.*, **1**, 361 (1978); https://doi.org/10.1111/j.1745-4514.1978.tb00193.x
21. M. Dubois, K.A. Gilles, J.K. Hamilton, P.A. Rebers and F. Smith, *Anal. Chem.*, **28**, 350 (1956); https://doi.org/10.1021/ac60111a017
22. A.B. Blakeney, P.J. Harris, R.J. Henry and B.A. Stone, *Carbohydr. Res.*, **113**, 291 (1983); https://doi.org/10.1016/0008-6215(83)88244-5
23. K. Chattopadhyay, C.G. Mateu, P. Mandal, C.A. Pujol, E.B. Damonte and B. Ray, *Phytochemistry*, **68**, 1428 (2007); https://doi.org/10.1016/j.phytochem.2007.02.008
24. W.S. York, A.G. Darvill, M. McNeil, T.T. Stevenson and P. Albersheim, *Methods Enzymol.*, **118**, 3 (1986); https://doi.org/10.1016/0076-6879(86)18062-1
25. J.S. Craigie, Z.C. Wen and J.P. van der Meer, *Bot. Mar.*, **27**, 55 (1984); https://doi.org/10.1515/botm.1984.27.2.55
26. C. Rochas, M. Lahaye and W. Yaphe, *Bot. Mar.*, **29**, 335 (1986); https://doi.org/10.1515/botm.1986.29.4.335
27. S.C. Fry, The Growing Plant Cell Wall: Chemical and Metabolic Analysis, Longman Scientific and Technical, Longman Group UK Ltd, pp. 135 (1988).
28. T.T. Stevenson and R.H. Furneaux, *Carbohydr. Res.*, **210**, 277 (1991); https://doi.org/10.1016/0008-6215(91)80129-B
29. A.B. Blakeney and B.A. Stone, *Carbohydr. Res.*, **140**, 319 (1985); https://doi.org/10.1016/0008-6215(85)85132-6
30. B. Ray and M. Lahaye, *Carbohydr. Polym.*, **66**, 408 (2006); https://doi.org/10.1016/j.carbpol.2006.03.027
31. A.D. Becke, *J. Chem. Phys.*, **98**, 5648 (1993); https://doi.org/10.1063/1.464913
32. C. Lee, W. Yang and R.G. Parr, *Phys. Rev. B Condens. Matter*, **37**, 785 (1988); https://doi.org/10.1103/PhysRevB.37.785
33. T.T.V. Tran, B.T. Huy, H.B. Truong, M.L. Bui, T.T.T. Thanh and D.Q. Dao, *Monatsh. Chem.*, **149**, 197 (2018); https://doi.org/10.1007/s00706-017-2056-z
34. M.W. Lodewyk, M.R. Siebert and D.J. Tantillo, *Chem. Rev.*, **112**, 1839 (2012); https://doi.org/10.1021/cr200106v
35. R.G. Parr and W. Yang, Density Functional Theory of Atoms and Molecules, Oxford University Press: New York (1989).
36. L. Domingo, M. Ríos-Gutiérrez and P. Pérez, *Molecules*, **21**, 748 (2016); https://doi.org/10.3390/molecules21060748
37. M.J. Frisch, G.W. Trucks, H.B. Schlegel, G.E. Scuseria, M.A. Robb, J.R. Cheeseman, J.A. Montgomery Jr., T. Vreven, K.N. Kudin, J.C. Burant, J.M. Millam, S.S. Iyengar, J. Tomasi, V. Barone, B. Mennucci, M. Cossi, G. Scalmani, N. Rega, G.A. Petersson, N. Nakatsuji, M. Hada, M. Ehara, K. Toyota, R. Fukuda, J. Hasegawa, M. Ishida, T. Nakajima, Y. Honda, O. Kitao, H. Nakai, M. Klene, X. Li, J.E. Knox, H.P. Hratchian, J.B. Cross, V. Bakken, C. Adamo, J. Jaramillo, R. Gomperts, R.E. Stratmann, O. Yazyev, A.J. Austin, R. Cammi, C. Pomelli, J.W. Ochterski, P.Y. Ayala, K. Morokuma, G.A. Voth, P. Salvador, J.J. Dannenberg, V.G. Zakrzewski, S. Dapprich, A.D. Daniels, M.C. Strain, O. Farkas, D.K. Malick, A.D. Rabuck, K. Raghavachari, J.B. Foresman, J.V. Ortiz, Q. Cui, A.G. Baboul, S. Clifford, J. Cioslowski, B.B. Stefanov, G. Liu, A. Liashenko, P. Piskorz, I. Komaromi, R.L. Martin, D.J. Fox, T. Keith, M.A. Al-Laham, C.Y. Peng, A. Nanayakkara, M. Challacombe, P.M.W. Gill, B. Johnson, W. Chen, M.W. Wong, C. Gonzalez and J.A. Pople, Gaussian, Inc.: Wallingford CT (2004).
38. A.A. Kolender, M.C. Matulewicz and A.S. Cerezo, *Carbohydr. Res.*, **273**, 179 (1995); https://doi.org/10.1016/0008-6215(95)00078-8
39. P. Mandal, C.A. Pujol, M.J. Carlucci, K. Chattopadhyay, E.B. Damonte and B. Ray, *Phytochemistry*, **69**, 2193 (2008); https://doi.org/10.1016/j.phytochem.2008.05.004
40. A.A. Kolender, C.A. Pujol, E.B. Damonte, M.C. Matulewicz and A.S. Cerezo, *Carbohydr. Res.*, **304**, 53 (1997); https://doi.org/10.1016/S0008-6215(97)00201-2
41. R. Falshaw and R.H. Furneaux, *Carbohydr. Res.*, **307**, 325 (1998); https://doi.org/10.1016/S0008-6215(98)00030-5
42. E. Percival and J.K. Wold, *J. Chem. Soc.*, 5459 (1963); https://doi.org/10.1039/jr9630005459
43. S. Mazumder, P.K. Ghosal, C.A. Pujol, M.J. Carlucci, E.B. Damonte and B. Ray, *Int. J. Biol. Macromol.*, **31**, 87 (2002); https://doi.org/10.1016/S0141-8130(02)00070-3
44. T. Ghosh, C.A. Pujol, E.B. Damonte, S. Sinha and B. Ray, *Antivir. Chem. Chemother.*, **19**, 235 (2009); https://doi.org/10.1177/095632020901900603